Straight Line Path Following for Formations of Underactuated Surface Vessels Under Influence of Constant Ocean Currents

M. Burger, A. Pavlov, E. Børhaug, K.Y. Pettersen

Abstract— The problem of path following and formation control for underactuated 3-degrees-of-freedom surface vessels in the presence of unknown ocean currents is considered. The proposed controllers make the vessels asymptotically constitute a desired formation that follows a given straight-line path with a desired speed profile. This control goal is achieved in the presence of currents of unknown direction and magnitude. The proposed controller consists of an adaptive yaw controller, which makes every vessel converge to its desired path, and a surge controller, which guarantees formation assembly along the path with the desired forward speed. The results are illustrated by simulations.

I. INTRODUCTION

Formation control of marine vessels is an enabling technology for a number of relevant applications. A fleet of multiple surface vessels moving together in a prescribed pattern can form an efficient data acquisition network for environmental monitoring, shallow water archaeological surveys, and oil and gas exploration. Moreover, formation control techniques can be used to perform underway replenishment at sea and to perform automated towing operations. In many cases the desired motion of a formation is characterised in terms of a geometric path to be followed and a desired along-the-path speed profile. For example, it is a common practice that the path is characterised by straight lines connecting way-points.

The path following control problem for a single marine vehicle has been investigated in a number of publications. In this paper we focus on control of underactuated surface vessels, for which the single vehicle control problem is considered in e.g. [5], [6], [10], [11]. Combining path following and formation control for a group of underactuated vessels adds a new level of complexity to the problem. Results on formation control can be found in a vast number of recent publications, see e.g. [13], [18] and references therein. Yet for marine vessels, especially in the underactuated case, one cannot simply put together general results on formation control (which are usually formulated on the kinematics level) and results on the path following problem for a single vehicle (studied both on the kinematics and dynamics level). Such a combination requires careful overall analysis due to the highly nonlinear dynamics of the systems involved, as pointed out in [3]. In [15] this analysis is done for the case of two cooperating vessels, and in [1], [4] it is performed for an arbitrary number of surface vessels.

The above mentioned papers do not take ocean currents into account. Yet, for accurate guidance of vessels, such disturbances should be dealt with in the controller design. For operations where the position of the vessel is important,

such as bathymetric mapping, environmental monitoring and archaeological surveys, the vessel formation should be able to follow its desired path closely, despite the disturbance of unknown currents, in order to obtain accurate measurement data. In [7] robust path following of an underactuated surface vessel is achieved using an adaptive control strategy, implementing a virtual ship approach. The result is based on a simplified vessel model without coupling between sway and yaw dynamics in both the mass and damping matrices. This approach was extended to the 3D case of AUVs in [8]. Dynamic positioning and way-point tracking of an AUV in the presence of ocean currents in the horizontal plane, which is similar to control of surface vessels, is discussed in [2], where the model has a diagonal mass matrix.

While the aforementioned papers considered control of a single vessel in the presence of ocean currents, already some work has been done on formation control including environmental disturbances. In [12] passivity properties and cascade connections are used to obtain global stability of a desired formation motion of fully actuated surface vessels.

In this paper we will consider the problem of path following and formation control for a group of underactuated surface vessels in the presence of unknown ocean currents. The surface vessels are modelled taking into account the inherent coupling of the yaw and sway dynamics. The solution proposed in this paper is a decentralised control strategy, in which line-of-sight (LOS) guidance is combined with adaptive control techniques. With this approach we obtain global asymptotic convergence of the vessels to the desired formation that follows a given straight-line path with a prescribed velocity profile. This work is an extension of [4] and [17], where the contribution of this paper is in adding robustness against ocean currents to the previous results.

The paper is organised as follows. In Section II the vessel model and control objectives are discussed. Section III starts with the assumptions used in this work, followed by the control laws for the vessels, and the theorem stating the main result of this paper. The proof of this theorem is given in Section IV. The performance of the obtained control laws is illustrated by simulations in Section V, while conclusions are drawn in Section VI.

II. VESSEL MODEL AND CONTROL OBJECTIVE

A. Vessel model

In this paper we consider a group of n surface vessels modelled by equations of the form [9]:

Norwegian University of Science and Technology, Department of Engineering Cybernetics, NO-7491, Trondheim, Norway. Email: *Mernout.Burger / Alexey.Pavlov / Even.Borhaug / Kristin.Y.Pettersen@itk.ntnu.no*

$$\dot{\eta} = \begin{bmatrix} \dot{x} \\ \dot{y} \\ \dot{\psi} \end{bmatrix} = R(\psi)\nu, \ R(\psi) = \begin{bmatrix} \cos(\psi) & -\sin(\psi) & 0 \\ \sin(\psi) & \cos(\psi) & 0 \\ 0 & 0 & 1 \end{bmatrix} \quad (1)$$

$$M\dot{\nu} + C_{\mathrm{R}}(\nu)\nu + C_{\mathrm{A}}(\nu_{\mathrm{r}})\nu_{\mathrm{r}} + D(|\nu_{\mathrm{r}}|)\nu_{\mathrm{r}} = f, \quad (2)$$

where $\eta = [x\ y\ \psi]^\top$ contains the positions x, y and orientation ψ of the vessel in an inertial coordinate frame, and the vector $\nu = [u\ v\ r]^\top$ contains the linear velocities u, v and the angular velocity r given in the body-fixed coordinate frame. The vessel's velocity relative to the water is given by $\nu_\mathrm{r} := \nu - \nu_\mathrm{c}$, where ν_c denotes the ocean current velocity expressed in the body-fixed frame. We assume the current is constant and irrotational in the inertial frame, giving

$$\nu_\mathrm{c} = R^\top(\psi) \begin{bmatrix} \rho \\ 0 \end{bmatrix}, \tag{3}$$

where $R^\top(\psi)$ is the transpose of the rotation matrix from the inertial to the body-fixed coordinate frame as defined in (1), and $\rho = [\rho_x\ \rho_y]^\top$. The vector $f = [f_u\ f_v\ f_r]^\top$ contains the control force in surge f_u, the rudder force $f_v = -Y_\delta \delta$ and moment $f_r = -N_\delta \delta$ affecting the sway and yaw dynamics respectively. Here δ denotes the rudder deflection, and $Y_\delta, N_\delta < 0$ are constant actuator parameters. The matrix $M = M^\top > 0$ is a mass matrix containing both the rigid-body and added mass components. The matrices $C_\mathrm{R}(\nu)$ and $C_\mathrm{A}(\nu_\mathrm{r})$ contain to the Coriolis and centripetal forces and moments for the rigid-body and added mass, respectively. The damping matrix $D(|\nu_\mathrm{r}|) = D + D_\mathrm{N}(|\nu_\mathrm{r}|)$ includes both linear and quadratic damping terms. In the controller design presented below, we use the simplified model

$$M\dot{\nu} + C(\nu)\nu + D\nu_\mathrm{r} = f, \tag{4}$$

where we approximate the sum $C_\mathrm{R}(\nu)\nu + C_\mathrm{A}(\nu_\mathrm{r})\nu_\mathrm{r}$ by $(C_\mathrm{R}(\nu)+C_\mathrm{A}(\nu))\nu = C(\nu)\nu$ and omit the quadratic damping term. Since the omitted term $D_\mathrm{N}(|\nu_\mathrm{r}|)\nu_\mathrm{r}$ provides additional damping, thereby enhancing the system stability, a stabilising controller designed for the simplified model (4) will also render the original system stable. For this reason the controller presented in this paper will be designed based on this simplified model. The adaptive nature of the controller will allow it to compensate for any constant offset due to the omitted/approximated terms. The performance of this controller will be tested in simulations for the original system (1)-(2). The structure of the matrices $M, C(\nu)$ and D is given by:

$$M = \begin{bmatrix} m_{11} & 0 & 0 \\ 0 & m_{22} & m_{23} \\ 0 & m_{23} & m_{33} \end{bmatrix}, \quad D = \begin{bmatrix} d_{11} & 0 & 0 \\ 0 & d_{22} & d_{23} \\ 0 & d_{32} & d_{33} \end{bmatrix},$$

$$C(\nu) = \begin{bmatrix} 0 & 0 & -m_{22}v - m_{23}r \\ 0 & 0 & m_{11}u \\ m_{22}v + m_{23}r & -m_{11}u & 0 \end{bmatrix}.$$

Notice that the system is underactuated, since there are only two independent control inputs f_u and δ to control the vessel in the three degrees of freedom: surge, sway and yaw.

For control purposes we use the total speed U, sideslip angle β, and course angle χ (see [5], [6]), given by

$$U := \sqrt{u^2 + v^2}, \quad \beta := \operatorname{atan2}(v; u), \quad \chi := \psi + \beta. \tag{5}$$

With a slight abuse of notation due to simplicity and space considerations, (1) can be rewritten as

$$\dot{x} = U\cos(\chi), \quad \dot{y} = U\sin(\chi), \quad \dot{\psi} = r. \tag{6}$$

Notice that this representation is well-defined for $u > 0$. Since the designed controller will be based on this model, special care will be taken to guarantee that the controller is well-defined, even for $u \le 0$.

The dynamics model is reformulated by multiplying both sides of (4) from the left by M^{-1}, which results in

$$\dot{u} = \mathcal{F}_u(\nu) + w_u^\top(\psi)\rho + \tau_u, \tag{7a}$$
$$\dot{v} = \mathcal{F}_v(\nu) + w_v^\top(\psi)\rho + \lambda\tau_r, \tag{7b}$$
$$\dot{r} = \mathcal{F}_r(\nu) + w_r^\top(\psi)\rho + \tau_r, \tag{7c}$$

where $\mathcal{F}_u(\nu)$, $\mathcal{F}_v(\nu)$ and $\mathcal{F}_r(\nu)$ are the functions containing the unforced system dynamics (see e.g. [11]), and $M^{-1}f = [\tau_u\ \lambda\tau_r\ \tau_r]^\top$ where λ is a constant, and there is a one-to-one relation between (τ_u, τ_r) and the original control inputs f_u and δ. We will consider (τ_u, τ_r) as the new control inputs to system (7). The sway dynamics (7b) is assumed to be inherently stable, with its boundedness properties captured by an assumption in the next section. The terms $w_*^\top(\psi)\rho$ are the corresponding components of the vector $M^{-1}D\nu_\mathrm{c}$, with ν_c given in (3). In what follows we will use the reformulated model (6)-(7) with (τ_u, τ_r) as control inputs and with the current vector $\rho = [\rho_x\ \rho_y]^\top \in \mathbb{R}^2$ as unknown parameters.

B. Control objective

In this paper we will design control laws for n vessels such that, after transients, the vessels constitute a desired formation and move along a desired straight-line path $\mathcal{P}$ with a given velocity profile $U_\mathrm{d}(t)$, as illustrated in Figure 1.
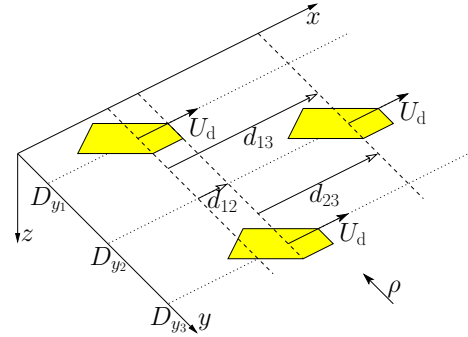

Fig. 1. Illustration of a desired formation motion.

This control goal must be achieved regardless of a constant yet unknown current, represented by the vector ρ. Notice that under the influence of a constant ocean current, after transients, the vehicles in the formation will move along the desired path with a non-zero sideslip angle in order to counteract the current.

By choosing the inertial coordinate system with the x-axis aligned with the desired path, the desired positions of the vessels in the formation are characterised by a set of desired distances D_{y_j} from the path $\mathcal{P}$ to the jth vessel, and by a set of desired distances δ_{ij} along the path $\mathcal{P}$ between the ith and the jth vessels (see Figure 1). The control objective can

then be formalised as

$$\lim_{t\to\infty} \quad y_j(t) - D_{y_j} = 0 \tag{8a}$$
$$\lim_{t\to\infty} \quad \chi_j(t) = 0 \tag{8b}$$
$$\lim_{t\to\infty} \quad x_j(t) - x_i(t) - \delta_{ji} = 0 \tag{8c}$$
$$\lim_{t\to\infty} \quad \dot{x}_j(t) - U_{\mathrm{d}}(t) = 0 \tag{8d}$$

where the subscripts i and j are used to denote the individual vessels; $i, j \in \{1, \ldots, n\}$. Moreover, it is required that after transients the surge speed satisfies $u_j(t) \in [u_{\min}, u_{\max}]$, where $u_{\min} > 0$ determines the minimal speed to maintain controllability in yaw, and $u_{\max}$ is the maximal speed of the vessel in surge.

III. MAIN RESULT

We first state some assumptions used for obtaining a solution to the control problem given in Section II-B.

Assumption 1: The current velocity vector ρ is constant, but with unknown direction and magnitude. It is assumed an upper bound $\|\rho\| \leq U_{\mathrm{c}}$ on the current's magnitude is known.

Assumption 2: It is assumed that for surge speed $u(t) \in [u_{\min}, u_{\max}]$, the sideslip angle $\beta(t)$, as defined in (5), satisfies $|\beta(t)| \leq \bar{\beta} < \frac{\pi}{2}$. This assumption means that for the given range of u the sway speed is bounded by some constant determined by $\bar{\beta}$.

Assumption 3: There exists $\epsilon > 0$ such that the desired along-path speed $U_{\mathrm{d}}(t)$ satisfies the constraints

$$\frac{u_{\min} + \epsilon}{\cos(\bar{\beta})} \leq U_{\mathrm{d}}(t) \leq u_{\max} - \epsilon, \tag{9}$$

This assumption will be used to ensure that after transients the desired speed along the path can be realised with a surge speed lying strictly within $[u_{\min}, u_{\max}]$.

A. Control laws

To fulfil the control goals (8) in the presence of unknown currents ρ, we will use line-of-sight (LOS) guidance combined with an adaptive control strategy. For the underactuated vessel we cannot control the sway speed directly, hence the control strategy must be designed to control the sway motion, in particular for achieving (8a), through the control of the yaw and surge motion. All vessels $j \in \{1, \ldots, n\}$ implement the same control laws, which are discussed next.

1) Yaw control: Figure 2 shows a single vessel with its desired path, and defines the variables used for LOS guidance. The LOS guidance scheme used in this paper is based on [5], [6]. In LOS guidance the controller will try to steer the total velocity vector of the vessel such that it points towards a position a distance $\Delta > 0$ ahead of the vessel along the desired path (see Figure 2). This results in the angle χ_{d} denoting the desired direction the vessel should move. Therefore the course of the vessel χ_j should be controlled to track the *desired course angle* $\chi_{\mathrm{d}j}$ given by

$$\chi_{\mathrm{d}j} = -\mathrm{atan}\left(\frac{e_j}{\Delta}\right), \quad e_j := y_j - D_{y_j}, \tag{10}$$

where e_j is the distance between the path and the vessel, called the *cross-track error*. When the cross-track error
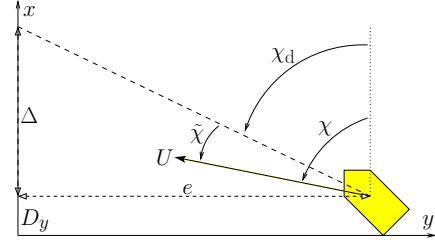

Fig. 2. Important angles and distances for line-of-sight guidance.

changes, also the desired course angle changes, and becomes zero when the vessel is on the path.

Using (5), we get the desired yaw angle $\psi_{\mathrm{d}j} := \chi_{\mathrm{d}j} - \beta_j$. Since β_j obtained by (5) is not well defined for all u_j, we will use a modified desired yaw angle given by

$$\psi_{\mathrm{d}j} = \chi_{\mathrm{d}j} - \beta_j^*, \tag{11}$$
$$\beta_j^* = \bar{\beta}\mathrm{sat}\left(\frac{1}{\bar{\beta}}\mathrm{atan}\left(\frac{v_j}{\max\{u_j, u_{\min}\}}\right)\right). \tag{12}$$

Notice that β_j^* is well defined for all u_j and v_j, it is globally bounded by $\bar{\beta}$, and it coincides with β_j when $u(t) \in [u_{\min}, u_{\max}]$. The latter follows from Assumption 2. To ensure the existence of time derivatives of β_j^*, one can use smooth variants of the saturation and maximum functions.

To achieve tracking of $\psi_{\mathrm{d}j}$ by ψ_j, we define the error variable $\tilde{\psi}_j := \psi_j - \psi_{\mathrm{d}j}$ and propose using

$$\tau_{r_j} = -\mathcal{F}_r(\nu_j) + \ddot{\psi}_{\mathrm{d}j} - k_\psi\tilde{\psi}_j - k_r\dot{\tilde{\psi}}_j - w_r^\top(\psi_j)\hat{\rho}_j, \tag{13}$$

where $k_\psi, k_r > 0$ are controller gains, and $\hat{\rho}_j$ is an estimate of the current vector ρ, which will be discussed later. By combining (7c), (13), and noticing $\ddot{\tilde{\psi}}_j = \dot{r}_j - \ddot{\psi}_{\mathrm{d}j}$, we obtain

$$\ddot{\tilde{\psi}}_j = -k_\psi\tilde{\psi}_j - k_r\dot{\tilde{\psi}}_j + w_r^\top(\psi_j)\tilde{\rho}_j, \tag{14}$$

from which it follows that for $\tilde{\rho}_j := \rho_j - \hat{\rho}_j = 0$ control law (13) can be seen as a feedback linearising controller.

2) Surge control: The surge control law used to accomplish the formation assembly (8c) with subsequent motion along the path with a desired speed (8d), is given by

$$\tau_{u_j} = -\mathcal{F}_u(\nu_j) + \dot{u}_{\mathrm{c}j} - k_u\tilde{u}_j - w_u^\top(\psi_j)\hat{\rho}_j, \tag{15}$$

where $k_u > 0$ is a controller gain, and

$$\tilde{u}_j = u_j - u_{\mathrm{c}j}, \tag{16a}$$
$$u_{\mathrm{c}j} = [U_{\mathrm{d}}(t) - g(\Sigma_j)]\cos(\beta_j^*), \tag{16b}$$
$$\Sigma_j = \sum_{i\in\mathcal{A}_j}(x_j - x_i - \delta_{ji}), \tag{16c}$$

Here $g(\Sigma_j)$ is a continuously differentiable saturation-like function, δ_{ji} is the desired distance in x-direction between vessels j and i (see Section II-B), $\mathcal{A}_j$ is the set of vessels with which vessel j has fixed bidirectional communication, for which we denote $\mathcal{G}$ as the communication graph with the vessels being nodes and the links corresponding to the bidirectional communication links. The function g is chosen as,

$$g(\Sigma_j) = \frac{2a}{\pi}\mathrm{atan}\left(\frac{\Sigma_j}{D_\Sigma}\right), \tag{17}$$

where $0 < a < \epsilon$ (see Assumption 3), and D_Σ is a tuning parameter used for adjusting the reactiveness on the error Σ_j.[1] Notice that $|g(\Sigma_j)| \leq a$, and $g(\Sigma_j) = \frac{a}{2}$ for $\Sigma_j = D_\Sigma$. By choosing U_d as in Assumption 3, using (16b), and defining $\varepsilon := \epsilon - a > 0$, we have

$$u_{\min} + \varepsilon \leq u_{cj} \leq u_{\max} - \varepsilon. \tag{18}$$

Combining (7a), (15) and (16a) gives the error dynamics

$$\dot{\tilde{u}}_j = -k_u \tilde{u}_j + w_u^\top(\psi_j)\tilde{\rho}_j. \tag{19}$$

3) Unknown parameter adaptation: Using the error vector $\xi_{1j} := [\tilde{u}_j \ \tilde{\psi}_j \ \dot{\tilde{\psi}}_j]^\top$, the error dynamics (14) and (19) can be written as

$$\begin{aligned}
\dot{\xi}_{1j} &= \begin{bmatrix} -k_u & 0 & 0 \\ 0 & 0 & 1 \\ 0 & -k_\psi & -k_r \end{bmatrix} \xi_{1j} + \begin{bmatrix} w_u^\top(\psi_j) \\ 0 \\ w_r^\top(\psi_j) \end{bmatrix} \tilde{\rho}_j \\
&= A\xi_{1j} + W^\top(\psi_j)\tilde{\rho}_j, \tag{20}
\end{aligned}$$

where 0 denotes a matrix of zeros of the appropriate size, and the matrix $W(\psi_j)$, introduced in (7), is given by

$$\begin{aligned}
W(\psi_j) &= \begin{bmatrix} w_u(\psi_j) & 0 & w_r(\psi_j) \end{bmatrix} \\
&= \begin{bmatrix} q_{11}\cos(\psi_j) & 0 & -q_{32}\sin(\psi_j) \\ q_{11}\sin(\psi_j) & 0 & q_{32}\cos(\psi_j) \end{bmatrix}, \tag{21}
\end{aligned}$$

with q_{11} and q_{32} defined by (see Section II-A)

$$Q := M^{-1}D = \begin{bmatrix} q_{11} & 0 & 0 \\ 0 & q_{22} & q_{23} \\ 0 & q_{32} & q_{33} \end{bmatrix}. \tag{22}$$

Since k_u, k_χ and k_r are positive, the matrix A in (20) is Hurwitz, and we can find a matrix P satisfying

$$P = \begin{bmatrix} p_1 & 0 & 0 \\ 0 & p_2 & p_3 \\ 0 & p_3 & p_4 \end{bmatrix} > 0, \ PA + A^\top P \leq -2\alpha I, \tag{23}$$

where $\alpha > 0$ is a design parameter, and I is the identity matrix of appropriate size. The adaptation law for the estimate of ρ_j (using $W = W(\psi_j)$) is chosen as

$$\dot{\hat{\rho}}_j = -\mu \left(\dot{W}P + WP\left[A + \mu W^\top WP\right] \right) \xi_{1j}, \tag{24}$$

where $\mu > 0$ is a tuning parameter, and

$$\dot{W}(\psi_j) = \begin{bmatrix} \frac{\partial w_u(\psi_j)}{\partial \psi_j} & 0 & \frac{\partial w_r(\psi_j)}{\partial \psi_j} \end{bmatrix} r_j. \tag{25}$$

B. Main result

We start by defining some constants, which will be used in the formulation and the proof of the main theorem:

$$\sigma_1 = \lambda_{\min}[WPW^\top] = \min\{p_1 q_{11}^2; p_4 q_{32}^2\} > 0, \tag{26}$$

$$\sigma_2 = \lambda_{\max}[(WP)^\top WP] = \max\{p_1^2 q_{11}^2; (p_3^2 + p_4^2)q_{32}^2\}, \tag{27}$$

where $\lambda_{\min}(\cdot)$ and $\lambda_{\max}(\cdot)$ denote the minimum and maximum eigenvalue of a symmetric matrix respectively, and p_* and q_* are given in (23) and (22). Due to the structure of $W(\psi_j)$ and P, these eigenvalues are constant and positive.

[1]With D_Σ one can take into account that e.g. $\Sigma_j = 10$ [m] of error is relatively 'larger' for a towing boat than for an oil tanker.

The main result of this paper is formulated in the following theorem:

Theorem 1: Consider n underactuated vessels modelled by (1) and (4), influenced by a constant ocean current of unknown direction and magnitude. Let the communication graph $\mathcal{G}$ be connected. Under Assumptions 1, 2 and 3, the control laws (13) and (15), combined with the adaptation law (24) in which the tuning parameter μ satisfies

$$0 < \mu < \frac{\alpha}{\sigma_2}, \tag{28}$$

guarantee that control goals (8) are achieved, and $u_j(t) \in [u_{\min}, u_{\max}]$ after transients.

IV. PROOF OF THEOREM 1

We begin our analysis by considering the path following behaviour of a single vessel. To ease the notations, we will omit the use of the subscript j in the first part of this section, and use $W = W(\psi)$ for notational compactness.

A. Tracking error dynamics

By defining the modified adaptation error variable $\lambda := \tilde{\rho} - \mu WP\xi_1$, we can write the error dynamics (20) as

$$\dot{\xi}_1 = A\xi_1 + \mu W^\top WP\xi_1 + W^\top \lambda. \tag{29}$$

The dynamics of the new variable λ are given by

$$\begin{aligned}
\dot{\lambda} &= \dot{\tilde{\rho}} - \mu \frac{d}{dt}(WP\xi_1) \\
&= \dot{\tilde{\rho}} - \mu WPW^\top \lambda \\
&\quad - \mu \left(\dot{W}P + WP\left[A + \mu W^\top WP\right] \right) \xi_1.
\end{aligned}$$

Since $\dot{\tilde{\rho}} := \dot{\rho} - \dot{\hat{\rho}} = -\dot{\hat{\rho}}$, with $\dot{\hat{\rho}}$ as given in (24), we obtain

$$\dot{\lambda} = -\mu WPW^\top \lambda. \tag{30}$$

Using the Lyapunov function candidate $\mathcal{V}_\lambda = \frac{1}{2}\lambda^\top \lambda$ gives

$$\dot{\mathcal{V}}_\lambda = -\mu \lambda^\top WPW^\top \lambda \leq -\mu \sigma_1 |\lambda|^2 < 0 \ \forall \ \lambda \neq 0, \tag{31}$$

where σ_1 is given in (26). Hence (30) is globally uniformly exponentially stable (GUES) for $\mu > 0$.

Consider the nominal system of (29) given by

$$\dot{\xi}_1 = (A + \mu W^\top WP)\xi_1.$$

Using the Lyapunov function candidate $\mathcal{V}_{\xi_1} = \frac{1}{2}\xi_1^\top P\xi_1$, where $P = P^\top > 0$ is defined in (23), we obtain

$$\begin{aligned}
\dot{\mathcal{V}}_{\xi_1} &= \xi_1^\top P(A + \mu W^\top WP)\xi_1 \\
&= \frac{1}{2}\xi_1^\top (PA + A^\top P)\xi_1 + \mu \xi_1^\top (WP)^\top WP\xi_1 \\
&\leq -\alpha|\xi_1|^2 + \mu \sigma_2 |\xi_1|^2, \tag{32}
\end{aligned}$$

where σ_2 is given in (27). By choosing $\mu < \frac{\alpha}{\sigma_2}$ we obtain that the nominal system is GUES. Hence (29) and (30) form a cascade connection of linear GUES systems. Using $\xi_2 := [\tilde{u} \ \tilde{\psi} \ \dot{\tilde{\psi}} \ \lambda^\top]^\top$, the cascade connection can be written as

$$\dot{\xi}_2 = \begin{bmatrix} \dot{\xi}_1 \\ \dot{\lambda} \end{bmatrix} = \begin{bmatrix} A + \mu W^\top WP & W^\top \\ 0 & -\mu WPW^\top \end{bmatrix} \xi_2. \tag{33}$$

Since the matrix $W^\top(\psi)$ is uniformly bounded, this implies that system (33) is GUES for $0 < \mu < \alpha/\sigma_2$.

The GUES property implies that there exists a ball $B_\delta = \{\xi_2 : ||\xi_2|| < \delta\}$ such that for any solution of (33) starting in $\xi_2(t_0) \in B_\delta$, the component $\tilde{u}$ of ξ_2 satisfies $|\tilde{u}(t)| < \varepsilon \ \forall \ t \geq t_0$. Due to GUES, any solution of (33) converges to B_δ in finite time; the rest of the analysis will be done for system (33) with initial conditions $\xi_2(t_0) \in B_\delta$. Notice that in this case, as follows from (18) and $u = u_{cj} + \tilde{u}$,

$$u(t) \in [u_{\min}, u_{\max}] \quad \forall \ t \geq t_0. \tag{34}$$

Due to Assumption 2 this implies $|\beta(t)| \leq \bar{\beta} < \frac{\pi}{2}$. This, in turn, due to the definition of β^* (see (12)), implies $\beta^*(t) = \beta(t)$ for $t \geq t_0$. Together with (11), this yields

$$\tilde{\chi} := \chi - \chi_d = (\psi + \beta) - (\psi_d + \beta^*) = \tilde{\psi}, \tag{35}$$

and the total speed $U = u/\cos(\beta)$ satisfies

$$|U| \leq \frac{u_{\max}}{\cos(\bar{\beta})} \quad \forall \ t \geq t_0. \tag{36}$$

We will use relations (34)-(36) in the subsequent stability analysis of the overall system.

B. Cross-track error dynamics

Using (35), $\dot{e} = \dot{y}$ given by (6) can be written as

$$
\begin{aligned}
\dot{e} &= U \sin(\chi) = U \sin(\chi_d) + U \left[\frac{\sin(\chi) - \sin(\chi_d)}{\chi - \chi_d} \right] \tilde{\chi} \\
&= U \sin(\chi_d) + U \cos(\chi') \tilde{\psi} \\
&= U \sin(\chi_d) + H_1(\chi, \chi_d, U, \xi_2)\xi_2,
\end{aligned}
$$

for some $\chi' \in [\chi, \chi_d]$ resulting from the mean value theorem. The function $H_1(\chi, \chi_d, U, \xi_2)\xi_2 := U \cos(\chi')\tilde{\chi}$ contains the term vanishing at $\xi_2 = 0$. Substituting χ_d from (10) gives

$$\dot{e} = -\frac{U}{\sqrt{\Delta^2 + e^2}} e + H_1(\chi, e, U, \xi_2)\xi_2, \tag{37}$$

where $||H_1(\chi, e, U, \xi_2)|| = |U \cos(\chi')| \leq u_{\max}/\cos(\bar{\beta})$, see (36). We will analyse system (37), (33) as a cascade of the nomimal system $\dot{e} = -Ue/\sqrt{\Delta^2 + e^2}$ with system (33) through the interconnection term $H_1(\chi, e, U, \xi_2)$. Using the Lyapunov function candidate $\mathcal{V}_e = \frac{1}{2}e^2$, and taking into account that $U(t) \geq u(t) \geq u_{\min} \ \forall \ t > t'$, we obtain

$$\dot{\mathcal{V}}_e = -\frac{U}{\sqrt{\Delta^2 + e^2}} e^2 \leq -\frac{u_{\min}}{\sqrt{\Delta^2 + e^2}} e^2 < 0 \ \forall \ e \neq 0,$$

and hence the nominal system is globally uniformly asymptotically stable (GUAS). For $|e| \leq \bar{e}$ we have

$$\dot{\mathcal{V}}_e = -\frac{u_{\min}}{\sqrt{\Delta^2 + \bar{e}^2}} e^2 < 0 \ \forall \ e \neq 0,$$

and hence the nominal system is also locally uniformly exponentially stable (LUES). Applying [16, Theorem 7 and Lemma 8], we conclude that the cascade system (37), (33) is exponentially stable in any ball of initial conditions.

From the definition of e in (10), we see that the control goal (8a) is met, and hence the vessel is guaranteed to converge to its desired path. Since $\chi := \chi_d + \tilde{\psi}$, and the fact that $\tilde{\psi} \to 0$ (33) and $e \to 0$ (37), this implies through (10) that control goal (8b) is also met.

C. Along-track dynamics

The foregoing part of this section shows the vessels will converge to their desired paths. It remains to prove that they will also constitute the desired formation along the path.

Notice that since $\cos \beta \geq \cos \bar{\beta} > 0$, there are no potential problems with division by zero in the following equations. Using (10), (16a) and (35), $\dot{x}$ in (6) can be rewritten as

$$
\begin{aligned}
\dot{x} &= U \cos(\chi) = U + U(\cos(\chi) - 1) \\
&= \frac{u}{\cos(\beta)} + \frac{u(\cos(\chi) - 1)}{\chi}(\{\chi - \chi_d\} + \chi_d) \\
&= \frac{u_c + \tilde{u}}{\cos(\beta)} + \frac{U(\cos(\chi) - 1)}{\chi} \left\{ \tilde{\psi} - \frac{\text{atan}\left(\frac{e}{\Delta}\right)}{e} e \right\} \\
&= \frac{u_c}{\cos(\beta)} + H_2(\chi, U, \xi_3)\xi_3, \tag{38}
\end{aligned}
$$

where $H_2(\chi, U, \xi_3)\xi_3$ contains all the terms vanishing at $\xi_3 := [\xi_2^\top \ e]^\top = 0$. Notice that since U is bounded, and all fractions in (38) are bounded, $||H_2(\chi, U, \xi_3)||$ is bounded. Combining (16b) and (38), and using subscripts to make a distinction between the variables for each vessel, we obtain

$$\dot{x}_j = U_d - g(\Sigma_j) + H_2(\chi_j, U_j, \xi_{3j})\xi_{3j}. \tag{39}$$

It has been shown in [4] that under the condition that the communication graph $\mathcal{G}$ is connected, solutions of system (39) for all $j \in \{1, \ldots, n\}$, in cascade with the ξ_{3j} dynamics of all the vessels (which are exponentially stable in any ball of initial conditions), satisfy control goal (8c). Moreover, since (8c) holds, $g(\Sigma_j)$ will also converge to zero. Since Σ_j, (33), (37) and ξ_{3j} converge to zero, (39) implies that (8d) is achieved. This concludes the proof of Theorem 1.

V. EXAMPLE

The proposed control scheme is tested in simulations for a formation of three underactuated surface vessels, using the full model (1)-(2). The ship model used in the simulation is CybershipII; a 1:70 scale model of an offshore supply vessel with a mass of 23.8 [kg] (see e.g. [14] for more details).

The desired formation is an equilateral triangle with its sides equal to 4 [m]. The desired straight-line path coincides with the x-axis, with $U_d(t) = 0.6$ [m/s]. The initial vessel poses $\eta_j = (x_j; y_j; \psi_j)$ [m; m; rad] are given by $\eta_1 = (2; 5; \frac{\pi}{6})$, $\eta_2 = (-2; 0; 0)$, and $\eta_3 = (0; -5; -\frac{\pi}{6})$.

All vessels have an initial surge speed of 0.5 [m/s]. The current velocity vector is given by $\rho = [-0.2 \ -0.2]^\top$, and $U_c = 0.3$ [m/s]. The used controller gains obtained by tuning are given by $k_\chi = 0.9$, $k_r = 3.3$, $k_u = 0.3$. The remaining parameter values are $\alpha = 5$, $\Delta = 3.5$ [m], $D_\Sigma = 3.5$ [m], and $a = 0.2$ [m/s]. For these values we obtain $\sigma_1 = 0.011$, $\sigma_2 = 0.165$, and choose $\mu = 15.0 \leq \frac{\alpha}{\sigma_2} = 30.3$ to satisfy the conditions of Theorem 1. The communication graph $\mathcal{G}$ is fully connected.

Figure 3 shows the movement of the vessels in the inertial reference frame for a simulation time of 60 [s]. The horizontal and vertical axis give the position in x-direction and y-direction respectively. Vessels are drawn at 10 [s] intervals, with striped lines drawn between the vessels to show the temporal formation structure. As can be seen from the figure, the vessels converge to the path and align in formation as expected. Notice that the heading ψ of the vessels is not
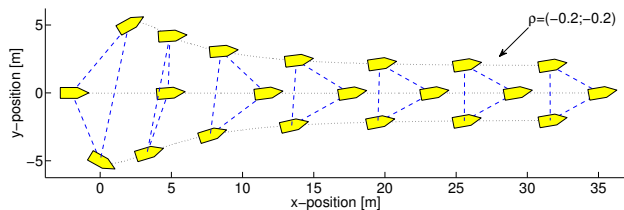
Fig. 3. Path following and synchronisation for a formation of three vessels.

aligned with the path, but the course χ is. This can also be seen in the left plot of Figure 4, which shows that the steady state heading angle is $\psi = 0.17$ [rad].
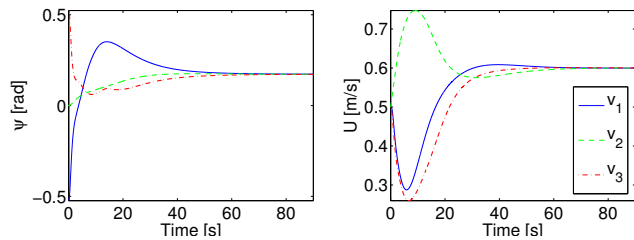

Fig. 4. Heading angle $\psi(t)$ *(left)* and total speed $U(t)$ *(right)* during path following and formation synchronisation.

The right plot of Figure 4 shows the total speed given by $U(t) = \sqrt{u^2(t) + v^2(t)}$. First the speeds of the three vessels differ, in order to synchronise with each other. When the formation is formed, the three speeds become equal to the desired along-path speed $U_d(t) = 0.6$ [m/s].
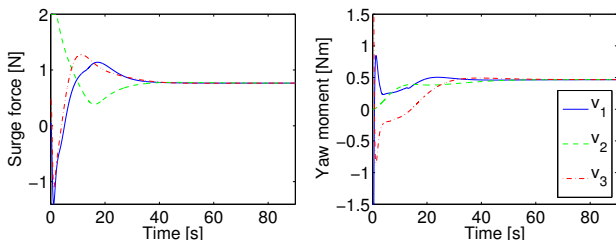

Fig. 5. Surge force $f_u(t)$ *(left)* and yaw moment $f_r(t)$ *(right)* during path following and synchronisation.

Figure 5 shows the forces and moments produced by the vessels in order to follow their trajectories. They are saturated at $-2.0 \leq f_u \leq 2.0$ [N] and $-1.5 \leq f_r \leq 1.5$ [Nm], which shows in the first few seconds. After this time, the control signals converge to a constant value, equal for all vessels.

VI. CONCLUSIONS

In this paper we have considered the problem of combined path following control and formation control for underactuated surface vessels in the presence of an ocean current of unknown direction and magnitude. The proposed controllers are based on line-of-sight guidance, adaptive control, and cascaded systems theory. The controllers guarantee asymptotic convergence of the vessels to a desired formation, and tracking of a desired speed reference along the desired path. This result is achieved without the need to measure the ocean current directly. Despite the use of a simplified model, the control strategy works on full model vessels, as confirmed by numerical simulations in Matlab. This control method does not take collision avoidance into account. In order to guarantee safe formation control, this should be included, and it is a topic for further research.

VII. ACKNOWLEDGEMENT

REFERENCES

[1] A.P. Aguiar, R. Ghabcheloo, A. Pascoal, C. Silvestre, J. Hespanha, and I. Kaminer. Coordinated path-following of multiple underactuated autonomous vehicles with bidirectional communication constraints. In *Proceedings of the 2nd International Symposium on Communications, Control and Signal Processing*, Morocco, March 2006.

[2] A.P. Aguiar and A.M. Pascoal. Dynamic positioning and way-point tracking of underactuated AUVs in the presence of ocean currents. *International Journal of Control*, 80(7):1092–1108, July 2007.

[3] E. Børhaug, A. Pavlov, and K.Y. Pettersen. Cross-track formation control of underactuated autonomous underwater vehicles. In *Group Coordination and Cooperative Control*, pages 35–54. Springer Verlag, 2006.

[4] E. Børhaug, A. Pavlov, and K.Y. Pettersen. Cross-track formation control of underactuated surface vessels. In *Proceedings of the 45th IEEE Conference on Decision and Control*, pages 5955–5961, December 2006.

[5] M. Breivik and T.I. Fossen. Path following for marine surface vessels. In *Proceedings of the OTO'04*, pages 2282–2289, Kobe, Japan, November 2004.

[6] M. Breivik and T.I. Fossen. Path following of straight lines and circles for marine surface vessels. In *Proceedings of the 6th IFAC Control Applications in Marine Systems (CAMS)*, pages 65–70, Ancona, Italy, July 2004.

[7] K.D. Do, Z.P. Jiang, and J. Pan. Robust adaptive path following of underactuated ships. *Automatica*, 40:929–944, 2004.

[8] K.D. Do, J. Pan, and Z.P. Jiang. Robust adaptive path following of underactuated autonomous underwater vehicles. *Ocean Engineering*, 31:1967–1997, 2004.

[9] T.I. Fossen. *Marine Control Systems - Guidance, Navigation and Control of Ships, Rigs and Underwater Vehicles*. Marine Cybernetics, 3rd edition, 2002.

[10] T.I. Fossen, M. Breivik, and R. Skjetne. Line-of-sight path following of underactuated marine craft. In *Proc. 6th IFAC Manoeuvring and Control of Marine Craft (MCMC)*, pages 244–249, Girona, Spain, September 2003.

[11] E. Fredriksen and K.Y. Pettersen. Global κ-exponential way-point maneuvering of ships: Theory and experiments. *Automatica*, 42(4):677–687, April 2006.

[12] I.-A.F. Ihle, M. Arcak, and T.I. Fossen. Passivity-based design for synchronized path-following. *Automatica*, 43:1508–1518, 2007.

[13] V. Kumar, N. Leonard, and A.S. Morse. *Cooperative Control*. Springer-Verlag, 2005.

[14] E. Kyrkjebø. *Motion Coordination of Mechanical Systems*. PhD thesis, Norwegian University of Science and Technology (NTNU), 2007.

[15] L. Lapierre, D. Soetanto, and A. Pascoal. Coordinated motion control of marine robots. In *Proc. 6th IFAC Manoeuvring and Control of Marine Craft (MCMC)*, Girona, Spain, September 2003.

[16] E. Panteley, E. Lefeber, A. Loria, , and H. Nijmeijer. Exponential tracking control of mobile car using a cascaded approach. In *Proc. IFAC Workshop on Motion Control*, pages 221–226, Grenoble, France, 1998.

[17] A. Pavlov, E. Børhaug, E. Panteley, and K.Y. Pettersen. Straight line path following for formations of underactuated surface vessels. In *Proceedings of 7th IFAC Symposyum on Nonlinear Control Systems*, Pretoria, South Africa, 2007.

[18] K.Y. Pettersen, J.T. Gravdahl, and H. Nijmeijer. *Group Coordination and Cooperative Control*, volume 336 of *Lecture Notes in Control and Information Sciences*. Springer, 2006.